

Electronic states and binding energies in ZnS-ZnSe superlattices

B. Gil, T. Cloitre, M. Di Blasio, P. Bigenwald, L. Aigouy, N. Briot,
O. Briot, D. Bouchara, R. L. Aulombard, and J. Calas

Université Montpellier II, Groupe d'Etudes des Semiconducteurs, Case courrier 074, 34095 Montpellier Cedex 5, France

(Received 31 May 1994; revised manuscript received 8 August 1994)

We present a detailed study of the optical properties of short-period ZnS-ZnSe strained-layer superlattices. These superlattices have been grown by metalorganic vapor-phase epitaxy. We show that the photoluminescence exhibits a low-energy tail due to localization of the exciton to interfacial potential fluctuations. A detailed analysis of the electronic structure has been performed using the envelope-function approach to obtain the valence-band and conduction-band envelope functions and band lineups. This was completed by a self-consistent calculation of the exciton binding energies. In this calculation the marginal conduction-band offset deduced from the standard envelope-function calculation is corrected by the electrostatic deformation produced by the presence of a localized hole wave function.

I. INTRODUCTION

Superlattices (SL's) are multilayer artificial compounds made up of successive depositions of thin metals, insulators, and semiconductors layers. In relation with the progress made during the last decades in the preparation of high purity materials, together with the advent of modern growth techniques, high crystalline quality and chemically pure compounds can now be synthesized. As a consequence, thin individual layers of different physical properties can be linked in a periodic manner along the growth axis. This has led to a tremendous development in the investigation of the properties of superlattices at the international level.^{1,2} In the field of semiconductors, SL's have been (and still are) grown from group IV elements (Si-Ge SL's), or from various III-V or II-VI compounds. Apart from Si-based applications, the majority of SL's are made up of GaAs and its different combinations of indium- and aluminium-based alloys.³ Besides III-V compounds, minor interest has been devoted to research on II-VI compounds (except for mercury-cadmium telluride), because the band gap of tellurium-related compounds are comparable to those of the III-V family. Thus, only an interest concerning wide band gap II-VI compounds that are selenium- and sulphur-based remained. The possibility to make a *p-n* junction by *p*-doping ZnSe was demonstrated with the growth of samples by molecular-beam epitaxy (MBE).^{4,5} Several II-VI bright-light emitters (including LED's and lasers) based on MBE-grown *p*-type ZnSe crystals, operating in the upper part of the visible spectrum have been fabricated for the last three years.^{6,7}

The theme that this paper will address is the optical properties of ZnS-ZnSe superlattices which are expected to be promising candidates for nonlinear optics.⁸⁻¹¹ We have grown short-period ZnS-ZnSe strained-layer superlattices (SLS's) by metalorganic vapor-beam epitaxy (MOCVD). These superlattices are grown as 45 repeated basic building blocks, where the thickness of the well and barrier widths are varied from 8 up to 25 Å. These SLS's were grown with a ZnSe buffer. The following optical ex-

periments were performed: reflectivity, photoreflectance, and photoluminescence (PL) at pumped liquid-helium temperature (2 K). From these experiments, we could detect the signatures of the heavy- and light-hole excitons. By using a marginal conduction-band offset in an elementary envelope-function calculation, we have been provided with a fairly good correlation between the theoretical and experimental data. A self-consistent calculation of the exciton binding energies has been performed. In this self-consistent calculation, we have included the electrostatic deformation of the marginal electron potential produced by the presence of a localized hole wave function. This reinforces the oscillator strength with respect to what we obtained when performing more conventional calculations of the exciton binding energy in low-dimensional semiconductor systems, and gives evidence of the sensitivity of the electronic structure of such superlattices to the presence of photoinduced electron-hole pairs.

II. SAMPLE GROWTH

The samples studied in this paper were grown using an ASM OMR 12 low-pressure MOVPE equipment, with a classical horizontal reactor. We have paid particular attention, together with Epichem Ltd., on the precursors. The growth of ZnS-ZnSe superlattices requires a set of precursors completing three main requirements over the classical ones: (i) high purity, (ii) low-growth-temperature ability to avoid interdiffusion at the interfaces (the optimum growth temperature may be low and very similar for the two materials), and (iii) no pre-reaction may occur between element II and element VI sources in order to obtain high uniformity layers and smooth interfaces. There are very few precursors exhibiting such properties, and to date, the only available combination completing all these conditions consists in the hydrides H₂Se and H₂S for the VI elements, combined with an adduct of dimethylzinc (DMZn) for the zinc precursor. The DMZn adduct we used in the present study is the tetramethylmethylenediamine dimethylzinc

(TMMD:DMZn) synthesized by Epichem Ltd. This colorless liquid precursor was purified by vacuum distillation and subsequent analysis by inductively coupled plasma emission spectroscopy failed to detect any metal contamination. Proton nuclear magnetic-resonance study ($^1\text{H NMR}$) have shown that this adduct is stoichiometric and does not dissociate during prolonged transport in a carrier gas. Both the vapor pressure and the $^1\text{H NMR}$ data were summarized in a previous paper.⁸ This DMZn adduct was successfully used in combination with H_2Se and H_2S to grow high quality ZnSe and ZnS single layers.¹² These preliminary studies allow us to obtain high thickness uniformity layers exhibiting mirrorlike morphologies linked to the very low level of premature reactions occurring when using H_2Se and H_2S with the TMMD:DMZn adduct.

The samples were deposited onto a (001) epi-ready GaAs wafer. Prior to the growth, the surface oxide was thermally desorbed from the substrate for 10 min at 580°C under hydrogen flow. The carrier gas was palladium purified hydrogen and the H_2 flow through the reactor was 3.3 standard liters per min during the growth experiments. The VI/II molar flow ratio was set to 5 during both ZnSe and ZnS layers growth. The precursor flows were set as follow: TMMD:DMZn = $30 \mu\text{mol}/\text{min}$, $\text{H}_2\text{S} = 150 \mu\text{mol}/\text{min}$, $\text{H}_2\text{Se} = 150 \mu\text{mol}/\text{min}$. All the samples were grown at $T_g = 300^\circ\text{C}$ and $P = 40$ Torr.

The structures consisted of a 45 period ZnS-ZnSe superlattices deposited onto a 3000 \AA thick ZnSe relaxed buffer layer. Growth interruptions of 10 sec were introduced between each layer deposition in order to improve the interfaces abruptness since such a procedure is of crucial importance as previously demonstrated for ZnSe-ZnTe superlattices.¹³ X-ray diffraction experiments allowed a precise determination of the period and mean lattice parameter of each samples, in which satellite peaks up to the second order were observed. A modeling of the period and mean lattice parameter versus individual monolayer numbers in the period was performed to deduce the thickness of each layer from the x-ray data. The measured thickness for both the barrier and the well materials was ranging from $8\text{--}25 \text{ \AA}$ for the samples studied in this paper. The interfaces roughness and morphology are assessed further in this paper from the interpretation of the optical characterizations.

III. OPTICAL CHARACTERIZATION

The optical characterization presented here has been made from 2 K up to room temperature using the 325-nm radiation of a He-Cd laser having 10 mW output pump power together with a 10-cm focal length lens. Under these conditions we worked in a *low injection regime*. Besides this, a 100-W quartz halogen tungsten lamp was used for reflectance and photoreflectance experiments. Results presented in this section of the paper correspond to 2 K data for short-period superlattices. Figure 1 displays typical PL (bottom) and photoreflectance (top) spectra measured at 2 K for a superlattice grown onto a relaxed 3000 \AA thick ZnSe buffer layer. (The critical thickness for the coherent growth of ZnSe on GaAs is in

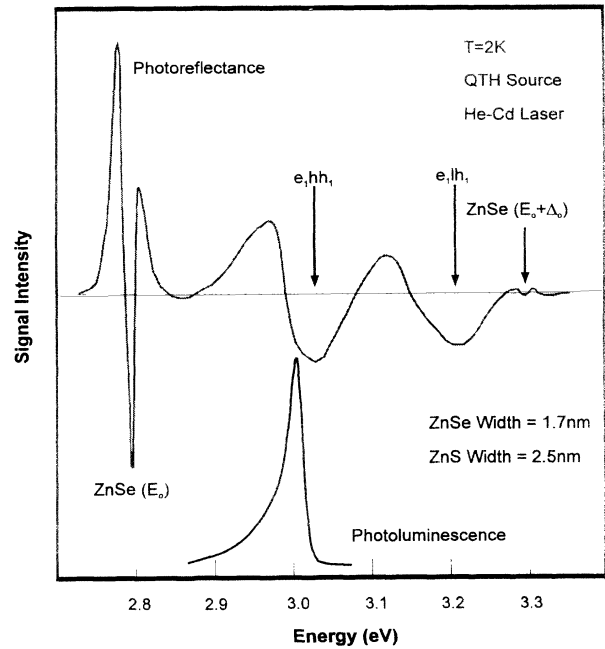


FIG. 1. Photoreflectance (top) and PL (bottom) of a ZnSe-ZnS superlattice grown on a GaAs substrates with a 3000-\AA ZnSe buffer layer. Clear signatures of transitions related to the superlattice and to the ZnSe buffer layer are identified. The PL line displays a low-energy tail due to existence of a weak interface disorder.

the region of 1500 \AA .) The PL line displays an asymmetric low-energy tail. Such line shape is commonly observed for such materials, as we will discuss further in this paper. The full width at half maximum (FWHM) is extremely good (32 meV) with a period of 4.2 nm , where the individual thicknesses of the ZnSe and ZnS layers are 1.7 and 2.5 nm , respectively. These values are in the range of what is reported in the literature for superlattices close to this design.^{14–31} The abruptness of the high-energy side permits us to make an accurate estimation of the PL energy, and a moderate Stokes shift (the energy relaxation of excitons before their recombination) is obtained between this data and the electron to heavy-hole feature of the photoreflectance spectrum.

This photoreflectance spectrum has a lot of information that can be resolved: starting from the lower energies, we respectively resolve the signatures of the E_0 transition in the ZnSe buffer layer, the e_1hh_1 exciton, its light-hole counterpart e_1lh_1 and the $E_0 + \Delta_0$ transition in the ZnSe buffer layer again. These spectroscopic results are consistent with a free-standing model of the strain state of the superlattices. In photoreflectance spectroscopy, we obtain the derivative spectra of an arbitrary order of the standard reflectivity spectra.³² Reflectivity changes are related to singularities of the dielectric constant around resonances. This dielectric constant can be basically modeled using a series of Drude-Lorentz oscillators centered around the resonant energies. The important parameters of this model are the resonant oscillator

strengths and dampings. The strengths of the derivative structures due to the contribution of the superlattice are important in the photoreflectance spectra. The contribution of the ZnSe buffer layer is narrower and stronger. Combined comparison of the intensities, widths of the superlattice related derivative structures, together with the ZnSe ones, leads us to conclude that the oscillator strengths of the heavy-hole and light-hole excitons confined in the superlattice are significantly increased with respect to bulk ZnSe free exciton. This is in relation with the important values of the binding energy in the superlattice.

We now present the evolution of the PL energy as a function of the superlattice design. Figure 2 displays 2 K PL data taken for superlattices having constant thickness of ZnS (barrier) layers. The effect induced by the thickness reduction of the ZnSe confining layer are illustrated in case of thick barrier layers in order to limit the effect of heavy-hole miniband formation when carrier tunneling between adjacent wells becomes important. We note two things: first, the PL energy increases when the thickness of the confining layer decreases. As we shall see in the next section of the paper, the strain state of the superlattice can vary from sample to sample. So, at this stage, we will limit the discussion to saying that we observe what is at first order expected for any type-I system when decreasing the thickness of the confining layer. The second point concerns the FWHM of the PL lines: we show in Fig. 2 that this quantity increases progressively as a function of the ZnSe well thickness from 24 to 32 and finally 42 meV.

This behavior is linked to the nature of the ZnS-ZnSe interface. First, we have to consider the possible syn-

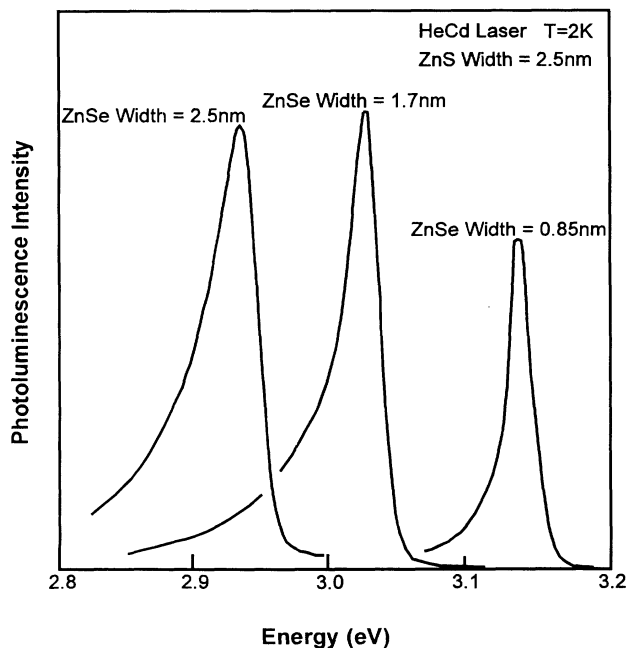


FIG. 2. PL spectra taken at 2 K on superlattices with constant thickness of ZnS. They display the blueshift of the emitted photon when the width of the ZnSe layers decreases.

thesis of Ga_2Se_3 compound at the II-VI-GaAs interface. This compound, which exhibits a strong lattice mismatch with ZnSe ($\sim 4\%$), may favor islanding at large distances of this interface.¹² Second, we note that, in the free-standing situation, the in-plane lattice parameter is intermediate between the values of the two bulk compounds. In fact, it can be expressed by a function of the relative thickness of the two compounds constituting the superlattice. For $a_{\text{ZnS}} = 5.4041 \text{ \AA}$ and $a_{\text{ZnSe}} = 5.6684 \text{ \AA}$, in the free-standing situation, the ZnS layers undergo a biaxial strain while the ZnSe layers undergo a biaxial compression. As the crystalline quality of biaxially stretched compounds is poor when compared to unstrained or biaxially compressed layers, we conclude that, the interface quality is poor, when ZnS layers are thinner than ZnSe layers. The spectra displayed on Fig. 3 are consistent with the following interpretation:

(i) The PL line shape is different when ZnS undergoes strong or weak biaxial stretching as shown by the three spectra reported on the figure.

(ii) We note the appearance of an intense additional line of extrinsic nature at a lower energy than that of the free exciton band. Using the more intense 350-nm radiation of an ionized argon laser, we could observe saturation of the intensity of this extrinsic line at high injection density.

(iii) The amount of elastic energy stored in the whole superlattice should also be considered when explaining the PL linewidth. This appears in Fig. 4 where are re-

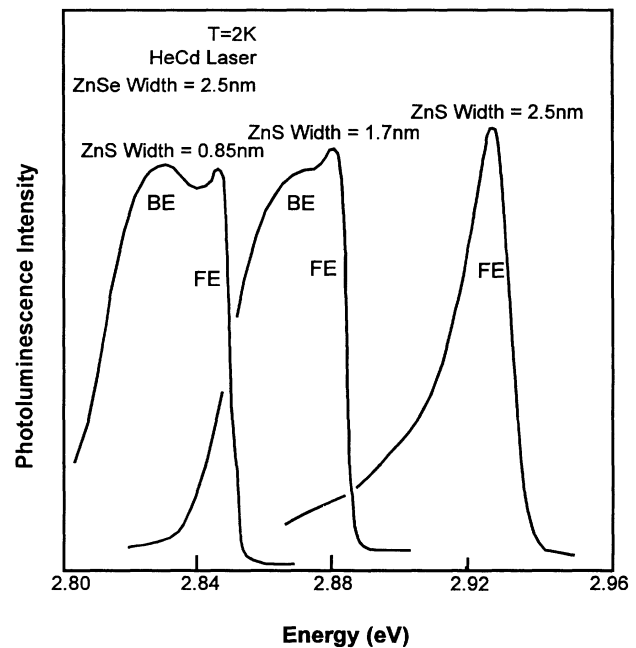


FIG. 3. PL spectra taken at 2 K which display the increase of the miniband formation and subsequent redshift of the band gap when the width of the barrier layers decreases and the width of the well is kept constant. Note the observation of extrinsic recombination at the low-energy part of the spectra (see text for details).

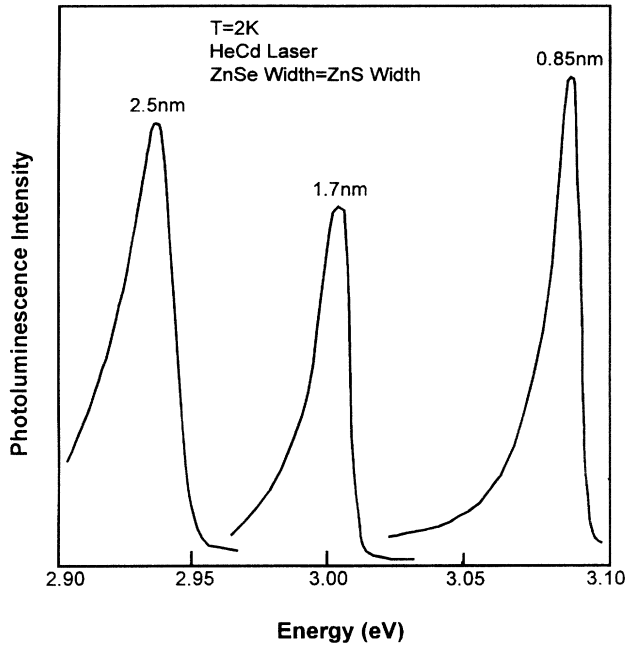


FIG. 4. Blueshift of the PL observed for superlattices having identical thicknesses of ZnS and ZnSe when the period diminishes.

ported some PL data taken for samples having identical ZnS and ZnSe numbers of monolayers. Thus, elasticity theory predicts the superlattices to be in a same strain state. We note that the smaller the period, the sharper the PL.

Extensive works on conventional *unstrained* GaAs-(Ga,Al)As superlattices have shown that the PL line shape is related to the interface morphology.^{33,34} Interface imperfections such as random distributed islands or terraces have been frequently observed. High-quality samples grown on exactly oriented substrates give split sharp PL lines corresponding to exciton confinement in layers of well-defined thickness with lateral extension L_T larger than the Bohr exciton diameter D_{exc} (~ 250 Å in GaAs). Control of the terraces sizes has been made possible by growing such III-V samples on 2° or 4° tilted substrates (terraces sizes of 8 or 4 nm are, respectively, obtained). When $L_T \sim D_{exc}$, the excitons experience intralayer thickness fluctuation resulting in remarkable inhomogeneous broadening. With further decreasing of the size of the terraces, when $L_T \ll D_{exc}$, the excitons are no longer subject of inhomogeneous broadening and sharp unsplit luminescence band results since the exciton samples wells having in-plane modulated thickness. Strained-layer systems behave in a more complex manner since stretching and compression of some bonds lead to storage of large amounts of elastic energy in the epilayers. Increasing the thickness of the strained layers favors the onset of dislocation creation, could result in nonhomogeneous strain through the epilayer. Subsequently, interfaces obtained to date are generally not as smooth as for GaAs-(Ga,Al)As. In our samples, as no

splitting has been observed in the PL and reflectance spectra, we conclude that the in-plane Bohr exciton diameter (~ 50 Å) is approximately equal to or larger than the lateral extensions of interface imperfections. In our superlattices, as the interface are disordered, we have to consider the localization of excitons due to in-plane potential fluctuations. This phenomenon has been subject to continuous interest in bulk compounds since the works of Cohen and Sturge³⁵ and Permogorov *et al.*³⁶ on localization of excitons to three-dimensional potential fluctuations. In $Zn_xS_{1-x}Se$ alloys, for compositions close to the high-band-gap binary semiconductor, the low-temperature PL spectra are dominated by a broad asymmetric band located below the reflectance energy that gives the actual position of the band-gap edges.^{37,38} This band is interpreted as the recombination of the exciton in a tail of states associated with alloy fluctuations. At the low-band-gap composition range, the behavior of such alloys is different: the PL spectra show the usual donor and acceptor bound excitons recombination lines broadened by alloy fluctuations. When our superlattices have smooth interfaces, in other words when inter diffusion is small at the heterointerfaces, we have a low-energy tailed PL band with significant contribution of exciton scattering to weak interface disorder. This is similar to the PL of sulphur-rich alloy composition in $Zn_xS_{1-x}Se$ alloys.³⁸ we can also make the analogy with what is observed for GaAs-Ga_{1-x}Al_xAs in case of terrace extensions smaller than the exciton diameter D_{exc} .^{33,34} When the interface quality is lower, the inter diffusion is important at the heterointerfaces, and one has a situation similar to what was observed in bulk compounds Zn(S,Se) with significant alloys composition. It was shown that, instead of a PL tail, an additional line due to a bound exciton appears below the near-band-edge PL.³⁸ In our case, the strength of defects at the ZnS-ZnSe interfaces is sufficient to trap the excitons at low temperature. This is the GaAs-Ga_{1-x}Al_xAs-like situation where $L_T \sim D_{exc}$. This model indicates that the amount of disorder rules the width of the 2-K PL line, but also influences its temperature behavior and the exciton lifetimes. This is consistent with the lifetime measurements earlier published^{22,28} and with most of the temperature-dependent experiments reported in the literature. Detailed examination of the influence of the lattice temperature on the recombination mechanisms will be addressed in a forthcoming publication.

IV. STRAIN STATE AND ELECTRONIC STRUCTURE OF THE SUPERLATTICES

A. Basic equations

This section is devoted to the calculation of the electronic structure of the superlattices. This will be achieved within the context of the effective-mass approximation.^{39,40} The valence-band states can be calculated by taking into account of the mixing between light-hole and spin-orbit split-off hole in both the kinetic part and strain part of the valence states Hamiltonian. Due to the $\sim 5\%$ lattice mismatch between ZnSe and ZnS, these com-

pounds are subjected to important strain field. It has been shown elsewhere from a tight-binding approach of the electronic structure of strained-layer superlattices, that, interaction between valence- and high-conduction bands cannot be ruled out to interpret the optical properties of a comblike ZnTe-CdTe superlattice.⁴¹ Including this interaction in the envelope-function approach is *a priori* possible but requires a lot of additional parameters not yet available, so this effect will be neglected.

The valence-band Hamiltonian can be written as⁴²

$$H_v = H_{so} + H_{kin} + H_1 + H_2, \quad (1)$$

where H_{kin} and H_{so} are the kinetic and the spin-orbit Hamiltonian, respectively. H_1 is the orbital-strain Hamiltonian, H_2 is the stress-dependent spin-orbit Hamiltonian defined in Refs. 39, 40, and 42.

We look for solutions of the Schrödinger equation,

$$[H_v(z) + V_0(z)]F(z) = EF(z). \quad (2)$$

For the electron band, the envelope function, at $\mathbf{k}=0$ is easily obtained by solving a second-order differential equation of the kind

$$[-\partial/\partial z 1/m(z)\partial/\partial z + E_g(z) - V_0(z) + C(e_{xx} + e_{yy} + e_{zz})]\phi_\Gamma = E_\Gamma \phi_\Gamma. \quad (3)$$

C is the hydrostatic deformation potential of the Γ conduction extreme in the bulk semiconductor.

B. Strain state in the individual layers

While bulk ZnS and ZnSe are not lattice matched, an homomorphism will occur between the in-plane lattice parameters of the ZnS and of the ZnSe during the growth. As the thickness of the deposited II-VI compounds exceeds the critical thickness for coherent growth to GaAs, we can estimate the new in-plane lattice parameter of the superlattice $\langle a \rangle$ by minimizing the elastic energy stored at the superlattice period scale.⁴³ In this spirit, let us consider a cubic compound n with elastic constants s_{ij}^n , compliance constants C_{ij}^n , and lattice parameter a_n , N_n monolayers thick, biaxially strained perpendicularly to the (001) direction. The density of elastic energy stored in the layer is given by

$$\Delta W^n = \frac{1}{2} C_{11}^n [2(e_{xx})^2 + (e_{zz})^2] + C_{12}^n [2e_{xx}e_{zz} + (e_{xx})^2]. \quad (4)$$

The deformation components e_{ij}^n are expressed as a function of the in-plane parameter $\langle a \rangle$: $e_{xx}^n = \langle a \rangle / a^n - 1$, and $e_{zz}^n = -2(C_{12}^n / C_{11}^n) e_{xx}^n$. The magnitude of the built-in strain experienced by each layer is: $\sigma_n = e_{xx}^n (C_{11}^n - C_{12}^n)$.

The density of elastic energy stored in the layer of compound n can be expressed as a function of $\langle a \rangle$. Then $\langle a \rangle$ minimizes the total energy stored along a period of the superlattices $\Delta E = \sum_{n,m} N_n a_n (1 + e_{zz}^n) \Delta W^n$.

Figure 5 displays the splitting of the ZnS Γ_8 valence band as a function of the ratio $\Theta = n_{\text{ZnS}} / n_{\text{ZnSe}}$. Open diamonds correspond to the light-hole (Γ_7 symmetry in D_{2d}) and the full diamond line corresponds to the heavy-hole (Γ_6 symmetry in D_{2d}). The result of the calculation is also reported for ZnSe, open circles for the light hole, full

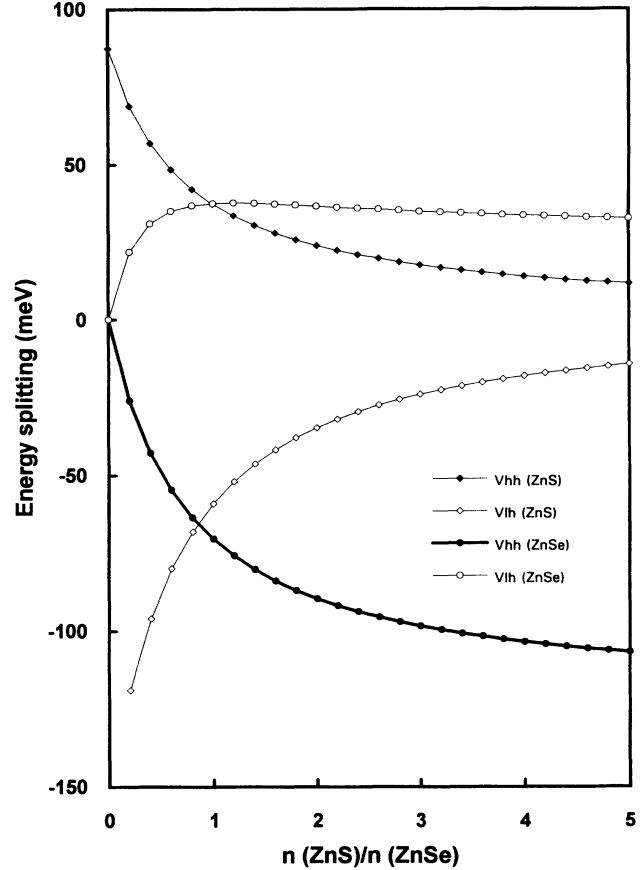


FIG. 5. Evolution of the splitting of the edges of the top most valence-band state of ZnSe and ZnS compounds within the context of a minimization of the elastic energy stored along a period of the superlattice. The data are expressed as a function of the relative thickness of the barrier and well width.

circles for the heavy hole. The splittings of both compounds are increasing when the amount of the other compound increases and shift in opposite manner depending on the sign of the strain (compression or tension). This is the expected trend. The saturation of the evolution of the light-hole level in ZnSe is related to the coupling with the spin-orbit split-off valence band under the biaxial compression whilst this does not appear for ZnS under biaxial dilatation.

C. Numerical calculations of the electronic structure of the superlattices

The quantity $V_0(z)$ that appears in Eqs. (2) and (3) is an adjustable parameter. This is the most important parameter of the calculation. We define the conduction-band offset as the whole contribution of both strain effects and of this “chemical” term. Most of the experimental and theoretical studies^{14,15,18,44–54} have concluded that the conduction-band lineup equals something like a tenth of the heavy-hole valence-band one. Roughly speaking let us say that we expect to have some 80-meV conduction-band lineup against 800-meV heavy-hole lineup.

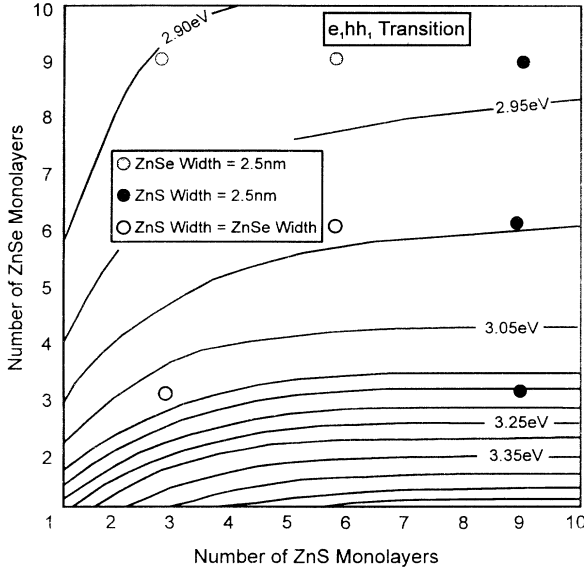


FIG. 6. Evolution of the fundamental electron to heavy-hole transition energy as a function of both ZnS and ZnSe thicknesses expressed in terms of monolayers numbers. Our sample positions are repaired using open circles.

Our experimental data could be fitted using a conduction-band chemical contribution of 220 meV. The full set of data is given on Table I, including the potential depths and miniband widths. We note that the conduction miniband continuously evolves from bulklike to superlatticelike behavior when increasing the thickness of the ZnS barrier layer. Except for sample 9/9, the electron state at minizone edge is resonant. In the 3/3 case, the heavy-hole miniband displays a significant dispersion whilst the other superlattices can almost be considered as

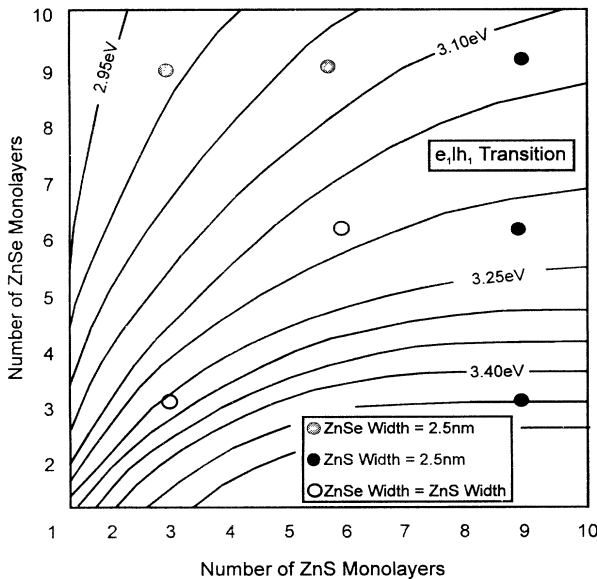


FIG. 7. The analogue of Fig. 6, but for the light-hole to electron transition energy.

multiple quantum wells for the hole.

This band to band calculation reproduces the whole set of data within some 40 meV for the electron to heavy-hole transitions. This is rather satisfactory for short-period strained-layer superlattices. The agreement is worse for the electron–light-hole transition may be because these transitions are broader and weaker in photoreflectance and because the electron-hole Coulomb interaction is larger. Figure 6 (respectively Fig. 7) displays the evolution of the constant energy curves for the electron to heavy-hole (respectively light-hole) transitions as well as positions of the samples.

D. Long-range exciton binding energy

The Coulomb interaction is important in wide gap bulk II-VI semiconductors. As in all type-I low-dimensional systems, the confinement should increase this binding energy.⁵⁵ The optical transitions are actually redshifted with respect to the values predicted from the band to band calculations. This interaction may even exceed the energy of the LO phonon (~ 31.3 meV in ZnSe). We have calculated it in the context of the variational approach using different trial functions in case of an isolated quantum well. In cylindrical coordinates, the Hamiltonian is

$$H = H_e + H_v + H_{ex} ,$$

$$H_{ex} = -\frac{\hbar^2}{2\mu} \left[\frac{\partial^2}{\partial \rho^2} + \frac{1}{\rho} \frac{\partial}{\partial \rho} \right] - \frac{e^2}{4\pi\epsilon_0\epsilon_r \sqrt{\rho^2 + z^2}} + \frac{1}{\rho^2} \frac{\partial^2}{\partial \theta^2} .$$

The solutions of the electron and hole contributions H_e and H_v have been obtained earlier in this section.

The eigenstates of the Schrödinger equation E are $E = E_e + E_h + E_b$. We have calculated the heavy-hole exciton binding energy. The electron and heavy-hole states and eigenfunction are obtained in the one-band approach. The exciton wave function is written as the product of the electron and hole envelope functions with an excitonic-like trial function. In cylindrical coordinates trial functions $\Phi_0(\rho, z_e, z_h) = \exp(-\rho/\lambda)$ and $\Phi_1(\rho, z_e, z_h) = \exp\{-[\rho^2 + \alpha^2(z_e - z_h)^2]/\lambda\}$ have been used. Parameters λ and α as variational parameters. In superlattices, the Rydberg energies are extremely complicated to calculate accurately. The problem has been addressed for GaAs-(Ga,Al)As superlattices where it has been shown that models of varying complexity have to be used depending on the well and barrier thicknesses, and miniband width.^{56–58} The experimental observation of the superlattice effect and its physical analysis has been addressed by Chomette *et al.*⁵⁹ for the GaAs-(GaAl)As combination. The exciton binding energies are intermediate between the two bulk values. At constant well width, the binding energy decreases with decreasing barrier width, when the superlattice effect increases. In this paper, to considerably simplify the numerical procedure, we have made the calculation for the single quantum well situation, which is valid when superlattices have

sufficiently thick barrier to prevent miniband formation. This approximation is almost fully valid if concerning the small or vanishing heavy-hole miniband dispersions in Table I. As this is not exactly the case for the electron, to strengthen this approximation, in the last part of the section, we perform a self-consistent calculation of the Rydberg starting from an arbitrary electron envelope function.

The result of the calculation appears in Fig. 8. For infinite wells, the second trial function is much more appropriate than the simplest one, particularly for large ZnSe layers. The result of this calculation differs from what has been announced by Hayashi and Katayama.⁶⁰ In calculating the same trend we find a sensitivity of the result to the trial function. Due to the lack of information concerning the intimate details of the calculation offered in Ref. 60, we are not able to analyze this in detail here. Exact computation (actually impossible to perform) should tend towards the bulk ZnSe value (20 meV) for extremely large ZnSe wells, and to the bulk ZnS value (29 meV) in the absence of a ZnSe layer. At best, this model predicts a Rydberg value to be about twice the bulk ZnSe one.

As the binding energy may be important compared with the electron confining potential, the expansion of the exciton wave function as the product of the electron and hole envelope functions solutions of a square-well problem, with an excitonlike trial function might not be appropriate since the localized hole wave function could deform the electron confining potential. This has been demonstrated for type-II band lineups with marginal valence potentials such as (Ga,In)As-GaAs (Ref. 61), CdTe-(Cd,Zn)Te (Ref. 62), or CdTe-(Cd,Mn)Te.⁶³ The resolution of the problem requires to perform a self-consistent calculation. We now adopt a more sophisticated formalism to describe the exciton. As previously suggested by Wu,⁶⁴ the wave functions of the two particles should be modified due to the Coulomb interaction between them. The importance of these corrections depends mostly on the degree of confinement of the particles: we expect little quantitative change on the eigenfunction of a strongly confined particle. For a particle having a confinement of the order of the exciton binding energy, the modifications cannot be neglected. In our case, the heavy and light hole can be considered as enough confined while the electron spreads in the barrier

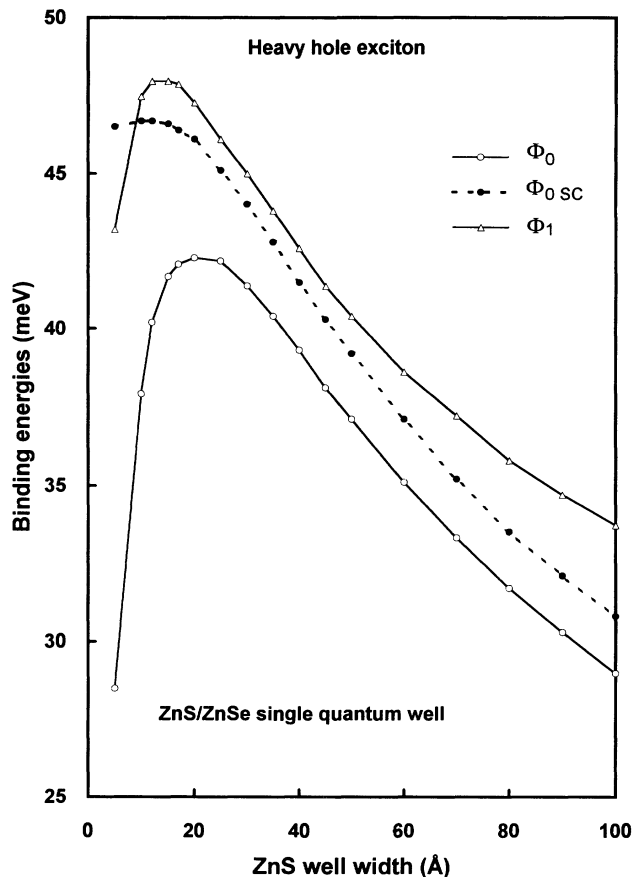


FIG. 8. Results of the variational calculation of the heavy-hole exciton in ZnSe-ZnS quantum wells. The calculation was made using two trial functions with one (Φ_0) and two (Φ_1) variational parameters. Besides this, the result of a self-consistent calculation with a one parameter trial function is also given (Φ_{osc}). See text for more details.

due to its low effective mass and to the feebly confining potential.

Making these assumptions, some of the previous equations are changed. In particular we write the total exciton wave function

$$\Phi(z_e, z_h, \rho) = \sqrt{2/\pi\lambda^2} \chi_h(z_h) f(z_e) e^{-\rho/\lambda},$$

TABLE I. Results of the envelope-function calculation as a function of the numbers of ZnS and ZnSe monolayers. The electron, heavy-hole, light-hole confining potentials V_i and miniband dispersions Δ_i are expressed in meV.

$N_{\text{ZnS}}/N_{\text{ZnSe}}$	V_e (meV)	V_{hh} (meV)	V_{lh} (meV)	Δ_e (meV)	Δ_{hh} (meV)	Δ_{lh} (meV)
3/3	83.1	834.5	615.1	519	33.5	302
3/6	83.5	824.1	604.3	228	6.1	91
3/9	83.7	818.5	597.7	132	2.3	41
6/3	82.8	844.1	623.2	212	2	80
6/6	83.1	834.5	615.1	116.17	0.3	22.4
6/9	83.3	828.3	609	72	0.1	9.4
9/3	82.6	848.6	626.4	113	0	22.8
9/6	82.9	840.3	620.3	64	0	4.8
9/9	83.1	834.5	615.1	41	0	1.8

with $f(z_e)$ being the corrected electron eigenfunction, satisfying a Schrödinger equation in which the potential term $V'_e(z_e)$ includes the interaction with the hole

$$\left[-\frac{\hbar^2}{2m_e} \frac{\partial^2}{\partial z_e^2} + V'_e(z_e) \right] f(z_e) = (E_e + E_b) f(z_e),$$

$$V'_e(z_e) = V_e(z_e) + \frac{\hbar^2}{2\mu\lambda^2} - \frac{e^2}{4\pi\epsilon_0\epsilon_r} \left[\frac{2}{\lambda} \right]$$

$$\times \int_{-\infty}^{2+\infty} \chi_h^2 dz_h \int_0^\infty \frac{e^{-2\rho/\lambda} \rho d\rho}{\sqrt{\rho^2 + z_{eh}^2}}.$$

The result of this third calculation appears on Fig. 8. This calculation gives intermediate values; it tends more rapidly than Φ_1 towards a bulk ZnSe-like value. As the envelope function for the electron is obtained from the knowledge of the heavy-hole one, this self-consistent calculation, which avoids the tedious calculations required to treat the exciton interaction in superlattices, is extremely reasonable for superlattices that exhibit electron miniband dispersion and no tunneling of the hole wave function between adjacent wells, which is the case of our superlattices. Subtracting this calculation to the band to band results brings the experimental results in better agreement with the calculation. We note that the light-hole exciton should not be as well described by using this model since the light-hole miniband dispersions are significant in our superlattices. To conclude, we wish to emphasize the fact that the Rydberg energies are larger than the Stokes shift we measure between photoreflectance and PL spectra. Moreover, this energy exceeds the average extension of the low-energy PL tail of the high energy peak of the PL, which means that localization effects to potential fluctuations can be easily counterbalanced by increasing the sample temperature.

V. CONCLUSION

We have grown ZnS-ZnSe strained-layer superlattices by MOVPE using a precursor TMMD which reduces premature reactions between precursors and gives good thickness uniformity of the epilayers. The superlattices have been characterized by x-ray analysis and optical spectroscopy. The PL has shown the existence of a weak interface disorder which results in the existence of a low-energy PL tail similarly to what was earlier observed in the literature. The width of the PL was found to be correlated to the amount of strain stored at the scale of the superlattice period and at the scale of the whole superlattice. Envelope-function calculations have enabled us to fit the whole set of data using a small conduction-band offset. We have calculated the heavy-hole exciton binding energy using a self-consistent approach taking into account of the electrostatic deformation of the marginal conduction-band potential produced by the localized hole. This binding energy exceeds both the LO-phonon energy and kT at room temperature. This weakens the LO dissociation channel and we may observe excitonic absorption even at room temperature.⁶⁵

ACKNOWLEDGMENTS

This work is partially supported by the Commission of the European Communities under contract "ESPRIT-BASIC RESEARCH MTVLE 6675. The "Groupe d'Etude des Semiconducteurs" is "Unité de Recherche Associée au CNRS No. 357." Dr. Bernard Gil acknowledges Dr. Catherine Gourdon, Dr. Yves Marfaing, and Dr. Henri Mariette for discussions concerning the mechanisms responsible for exciton localization in solid solutions based on II-VI and III-V compounds.

- ¹See, Phys. Today **46** (7) (1993), special issue on Optics of Nanostructures.
²C. Weisbuch and Borge Vinter, *Quantum Semiconductor Structures* (Academic, New York, 1993).
³A. B. Fowler, Phys. Today **46**, 59 (1993).
⁴M. Haase, J. Qiu, J. M. Depuydt, and H. Cheng, Appl. Phys. Lett. **59**, 1272 (1991).
⁵H. Jeon, J. Ding, W. Patterson, A. V. Nurmikko, W. Xie, D. C. Grillo, M. Kobayashi, and R. L. Gunshor, Appl. Phys. Lett. **59**, 3619 (1991).
⁶A. V. Nurmikko and R. L. Gunshor, IEEE J. Quantum Electron. **30**, 619 (1994).
⁷R. L. Gunshor and A. V. Nurmikko, IEEE J. Quantum Electron. **59**, 3159 (1994).
⁸J. Y. Zhang, X. W. Fan, S. Y. Wang, D. Z. Shen, and G. H. Fan, J. Cryst. Growth **117**, 523 (1992).
⁹X. W. Fan, D. Z. Shen, J. Y. Zhang, Z. P. Guan, and H. Tian, in *Proceedings of the 20th International Conference on the Physics of Semiconductors*, edited by E. M. Anastassakis and J. D. Joannopoulos (World Scientific, Singapore, 1991), p.

1016.

- ¹⁰T. Yokogawa, T. Saitoh, and T. Narusawa, Appl. Phys. Lett. **58**, 1754 (1991).
¹¹K. Yoshida, F. Minami, K. Inoue, and H. Fujiyasu, in *Proceedings of the 20th International Conference on the Physics of Semiconductors* (Ref. 9), p. 811.
¹²O. Briot, M. Di Blasio, T. Cloitre, N. Briot, P. Bigenwald, B. Gil, M. Averous, R. L. Aulombard, L. M. Smith, S. A. Rushworth, and A. C. Jones, in *Proceedings of the MRS Meeting, San Francisco, 1994* (Materials Research Society, Pittsburgh, in press).
¹³N. Briot, T. Cloitre, O. Briot, P. Boring, B. E. Ponga, B. Gil, R. L. Aulombard, M. Gailhanou, J. M. Salesse, and A. C. Jones, in *Electron Packaging Materials Science III*, edited by R. Jaccudine, K. A. Jackson, and R. C. Sundahl, MRS Symposia Proceedings No. 108 (Materials Research Society, Pittsburgh, 1993), p. 461.
¹⁴H. Kuwabara, H. Fujiyasu, H. Shimizu, A. Sasaki, and S. Yamada, J. Cryst. Growth **72**, 299 (1985).
¹⁵T. Yokogawa, M. Ogura, and T. Kajiwara, Appl. Phys. Lett.

- 49, 1702 (1986).
- ¹⁶T. Yokogawa, M. Ogura, and T. Kajiwara, *J. Appl. Phys.* **62**, 2843 (1987); T. Yokogawa, T. Fujita, M. Ogura, and T. Kajiwara, *J. Cryst. Growth* **93**, 708 (1988); T. Yokogawa, H. Sato, and M. Ogura, *J. Appl. Phys.* **64**, 5201 (1988); T. Yokogawa, T. Saitoh, and T. Narasawa, *J. Cryst. Growth* **101**, 550 (1990).
- ¹⁷Y. Yamada and T. Taguchi, *J. Cryst. Growth* **101**, 661 (1990).
- ¹⁸Y. Kawakami, T. Taguchi, A. Hiraki, *Technol. Rep. Osaka Univ.* **38-1921**, 109 (1988); *J. Cryst. Growth* **93**, 714 (1988).
- ¹⁹K. P. O'Donnell, P. J. Parbrook, B. Henderson, C. Trager-Cowan, X. Chen, F. Yang, M. P. Halsall, P. J. Wright, and B. Cockayne, *J. Cryst. Growth* **101**, 554 (1990).
- ²⁰T. Yao, M. Fujimoto, S. K. Chang, and H. Tanino, *J. Cryst. Growth* **111**, 823 (1991).
- ²¹A. Shen, H. Wang, Z. Wang, and S. Lu, *Appl. Phys. Lett.* **60**, 2640 (1992).
- ²²J. Cui, H. Wang, F. Gan, X. Huang, Z. Cai, Q. Li, and Z. Yu, *Appl. Phys. Lett.* **61**, 1540 (1992).
- ²³F. Yang, P. J. Parbrook, B. Henderson, K. P. O'Donnell, P. J. Wright, and B. Cockayne, *Appl. Phys. Lett.* **59**, 2142 (1991); K. P. O'Donnell, P. J. Parbrook, F. Yang, X. Chen, D. J. Irvine, C. Trager-Cowan, B. Henderson, P. J. Wright, and B. Cockayne, *J. Cryst. Growth* **117**, 497 (1992).
- ²⁴Z. P. Guan, J. H. Zhang, G. H. Fan, and X. W. Fan, *J. Cryst. Growth* **117**, 515 (1992).
- ²⁵J. Cui, H. Wang, and F. Gan, *J. Cryst. Growth* **117**, 505 (1992).
- ²⁶F. E. G. Guimaraes, J. Sollner, K. Marquardt, M. Heuken, and K. Heime, *J. Cryst. Growth* **117**, 1075 (1992).
- ²⁷C. Pong, F. Feigelson, and R. C. DeMattei, *J. Cryst. Growth* **128**, 650 (1993).
- ²⁸D. Oberhauser, W. Sack, C. Klingshirn, K. P. O'Donnell, P. J. Parbrook, P. J. Wright, and B. Cockayne, *Superlatt. Microstruct.* **9**, 107 (1991).
- ²⁹S. Hohnoki, S. Katayama, and A. Hasegawa, *Solid State Commun.* **89**, 41 (1994).
- ³⁰Shen Dezhen, Fan Xiwu, and Fan Guanghan, *Chin. Phys.* **12**, 758 (1992).
- ³¹Z. P. Guan, X. W. Fan, G. H. Fan, and X. R. Xu, *J. Lumin.* **45**, 224 (1990).
- ³²For a review see, O. J. Glemboki, *Proc. SPIE* **1286**, 2 (1990).
- ³³J. Massies, C. Deparis, C. Neri, G. Neu, Y. Chen, B. Gil, P. Auvray, and A. Regreny, *Appl. Phys. Lett.* **55**, 2605 (1989).
- ³⁴Y. Chen, J. Massies, G. Neu, C. Deparis, and B. Gil, *Solid State Commun.* **81**, 877 (1982).
- ³⁵E. Cohen and M. D. Sturge, *Phys. Rev. B* **25**, 3828 (1982).
- ³⁶S. Permogorov, A. Reznitzky, S. Verbin, G. O. Muller, P. Flogel, and M. Nikiforova, *Phys. Status Solidi B* **113**, 589 (1982).
- ³⁷D. Ouadjaout and Y. Marfaing, *Phys. Rev. B* **41**, 12096 (1990); **46**, 7908 (1992).
- ³⁸L. G. Suslina, D. L. Fedorov, S. G. Konnikov, F. F. Kodzhespirov, A. A. Andreev, and E. G. Sharlai, *Sov. Phys. Semicond.* **11**, 1132 (1977); R. Mach, L. G. Suslina, and A. G. Areshkin, *ibid.* **16**, 418 (1982).
- ³⁹B. Gil, P. Lefebvre, P. Boring, K. J. Moore, G. Duggan, and K. Woodbridge, *Phys. Rev. B* **44**, 1942 (1991).
- ⁴⁰B. Gil, L. K. Howard, D. J. Dunstan, P. Boring, and P. Lefebvre, *Phys. Rev. B* **46**, 3906 (1992).
- ⁴¹J. M. Jancu, D. Bertho, C. Jouanin, B. Gil, N. Pelekanos, N. Magnea, and H. Mariette, *Phys. Rev. B* **49**, 10802 (1994).
- ⁴²M. Chandrasekhar and F. H. Pollak, *Phys. Rev. B* **15**, 2127 (1977).
- ⁴³C. Mailhiot and D. L. Smith, in *Compound Semiconductor Strained-Layer Superlattices*, edited by R. M. Biefeld (Trans Tech Publications, Switzerland, 1989).
- ⁴⁴K. Shahzad, D. J. Olego, C. G. Van de Walle, *Phys. Rev. B* **38**, 1417 (1988).
- ⁴⁵C. G. Van de Walle and R. M. Martin, *Phys. Rev. B* **35**, 8154 (1987).
- ⁴⁶C. G. Van de Walle, *Phys. Rev. B* **39**, 1871 (1989).
- ⁴⁷C. Trager-Cowan, P. J. Parbrook, B. Henderson, and K. P. O'Donnell, *Semicond. Sci. Technol.* **7**, 536 (1992).
- ⁴⁸I. Gorczyca and N. E. Christensen, *Solid State Commun.* **72**, 785 (1989); *Phys. Rev. B* **44**, 1707 (1991).
- ⁴⁹D. Bertho and C. Jouanin, *Phys. Rev. B* **47**, 2184 (1993).
- ⁵⁰F. Minami, K. Yoshida, J. Gregus, K. Inoue, and H. Fujiyasu, in *Proceedings of the 2nd International Conference on Optics of Excitons in Confined Systems*, edited by A. d'Andrea, R. del Sole, R. Girlanda, and A. Quattropiani, IOP Conf. Proc. No. 123 (Institute of Physics and Physical Society, London, 1992), p. 249.
- ⁵¹Y. Yamada, Y. Masumoto, and T. Taguchi, *Surf. Sci.* **267**, 129 (1992); *J. Cryst. Growth* **117**, 484 (1992); Y. Yamada, Y. Masumoto, and K. Takemura, *Phys. Rev. B* **44**, 1801 (1991).
- ⁵²I. Gorczyca and N. E. Christensen, *Phys. Rev. B* **48**, 17202 (1993).
- ⁵³T. Nakayama, *J. Phys. Soc. Jpn.* **59**, 1029 (1990); *Proceedings of the 5th International Conference on High Pressure in Semiconductor Physics, Kyoto, 1992* [*Jpn. J. Appl. Phys.* **32**, 89 (1993)].
- ⁵⁴T. Taguchi, Y. Kawakami, and Y. Yamada, *Physica B* **191**, 23 (1993).
- ⁵⁵G. Bastard, E. E. Mendez, L. L. Chang, and L. Esaki, *Phys. Rev. B* **26**, 1974 (1982); R. L. Greene and K. K. Bajaj, *Solid State Commun.* **45**, 831 (1983); R. L. Greene, K. K. Bajaj, and D. E. Phelps, *Phys. Rev. B* **29**, 1807 (1984).
- ⁵⁶M. M. Dignan and J. E. Sipe, *Phys. Rev. B* **41**, 2865 (1990).
- ⁵⁷M. F. Pereira, Jr., I. Galbraith, S. W. Koch, and G. Duggan, *Phys. Rev. B* **42**, 8928 (1989).
- ⁵⁸P. Lefebvre, P. Christol, and H. Mathieu, *Phys. Rev. B* **46**, 13603 (1992).
- ⁵⁹A. Chomette, B. Lambert, B. Deveaud, F. Clérot, A. Régrény, and G. Bastard, *Europhys. Lett.* **4**, 461 (1987).
- ⁶⁰H. Hayashi and S. Katayama, *Phys. Rev. B* **39**, 8743 (1989).
- ⁶¹P. Bigenwald and B. Gil, *Solid State Commun.* **91**, 33 (1994).
- ⁶²E. Deleporte, G. Peter, J. M. Berroir, and C. Delalande, *Surf. Sci.* **267**, 137 (1992).
- ⁶³G. Peter, E. Deleporte, G. Bastard, J. M. Berroir, C. Delalande, B. Gil, J. M. Hong, and L. L. Chang, *J. Lumin.* **52**, 147 (1992); E. Deleporte, J. M. Berroir, G. Bastard, C. Delalande, J. M. Hong, and L. L. Chang, *Phys. Rev. B* **42**, 5891 (1990).
- ⁶⁴J. W. Wu, *Solid State Commun.* **67**, 911 (1988).
- ⁶⁵This is explained in detail in J. Ding, N. Pelekanos, A. V. Nurmikko, H. Luo, S. Samarth, and J. K. Furdyna, *Appl. Phys. Lett.* **57**, 2885 (1990).

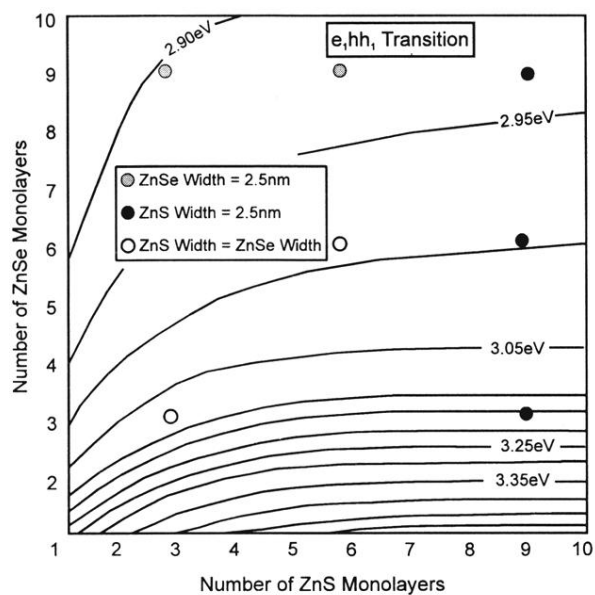


FIG. 6. Evolution of the fundamental electron to heavy-hole transition energy as a function of both ZnS and ZnSe thicknesses expressed in terms of monolayers numbers. Our sample positions are repaired using open circles.

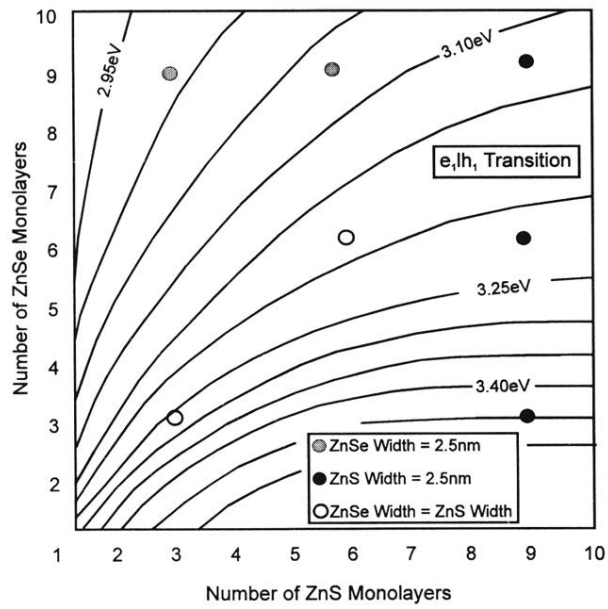


FIG. 7. The analogue of Fig. 6, but for the light-hole to electron transition energy.